Stanford Exploration Project, Report 120, May 3, 2005, pages 125–136

Common azimuth migration for elliptical and VTI media

Satyakee Sen and Biondo Biondi[1]

ABSTRACT

We derive the Commom Azimuth downward continuation operator for elliptically anisotropic and VTI media. For elliptically anisotropic media, the Common Azimuth downward continuation operator derived by a stationary phase approximation of the full 3-D downward continuation operator is exact and it agrees with the constraint imposed by the Common Azimuth approximation on the propagation direction of the source and receiver rays. For VTI media, the dispersion relationship is much more complicated and results in a quartic equation for the stationary path. We introduce a bounded form of Common Azimuth migration for this kind of media, which allows us to develop closed-form analytical solutions without directly solving the quartic equation. Error analysis indicates that the derived analytical solution has similar accuracy as that obtained by solving the full quartic equation. 3-D impulse responses of the anisotropic Common Azimuth downward continuation operator also show significant differences compared to the isotropic operator even at moderate propagation angles.

INTRODUCTION

Over the past several decades, anisotropy has been recognized as one of the important factors effecting the accuracy of seismic imaging methods. If anisotropy is not taken into account by wavefield extrapolation operators, subsurface reflectors (especially steeply dipping ones) will be mispositioned. Thus, incorporating anisotropy into existing isotropic wavefield continuation operators has gained significant importance over the past several years. Several methods have been developed to handle anisotropy which include both implicit and explicit extrapolation operators. These include anisotropic implicit methods (Ristow and Ruhl, 1997), anisotropic PSPI (Rousseau, 1997), explicit operators (Uzcategui, 1995), (Zhang et al., 2001), reference isotropic with explicit correction filters (Baumstein and Anderson, 2003) and explicit anisotropic correction filters (Shan and Biondi, 2004). However, no such method has been developed to incorporate anisotropy into the Common Azimuth migration operator. Common Azimuth migration (Biondi and Palacharla, 1996) is one of the most computationally effective wavefield continuation method for large 3-D marine surveys. The computational effectiveness of this method can be attributed to the stationary path approximation that this method uses which shrinks the computational volume for full 3-D wavefields from a five-dimensional space to a four-dimensional space. This greatly reduces the computations that are involved

[1]**email:** ssen@sep.stanford.edu, biondo@sep.stanford.edu

at each depth step. Thus, it would be extremely beneficial if anisotropy can be incorporated into the existing isotropic Common Azimuth migration downward continuation operator. In this paper, we develop a method for introducing anisotropy into Common Azimuth migration. In the following sections, we develop the anisotropic Common Azimuth migration operator, firstly for the relatively simple elliptically anisotropy media and then for the more complex VTI media. We then perform error analysis for our derived analytical solution for the VTI media and finally compare the 3-D impulse responses of the elliptically anisotropic Common Azimuth operator with that of the isotropic operator.

ELLIPTICAL ANISOTROPY

In this section, we derive the Common Azimuth downward continuation operator for an elliptically anisotropic media. The 3-D dispersion relation for VTI media given by Alkhalifah (1998) is:

$$k_z = \frac{\omega}{v}\sqrt{\frac{\frac{\omega^2}{v^2} - (k_x^2+k_y^2)(1+2\epsilon)}{\frac{\omega^2}{v^2} - 2(k_x^2+k_y^2)\eta(1+2\delta)}}, \tag{1}$$

where v is the vertical P wave velocity and $\mathbf{k}(k_x,k_y,k_z)$ is the wavenumber vector in Cartesian coordinates and ω is the circular frequency. The anisotropic parameters ϵ and δ are defined as:

$$\epsilon = \frac{C_{11}-C_{33}}{2C_{33}}, \delta = \frac{(C_{11}+C_{44})^2-(C_{33}-C_{44})^2}{2C_{33}(C_{33}-C_{44})}. \tag{2}$$

In deriving this dispersion relation it is assumed that the shear wave velocity is zero. This assumption holds for the remainder of this paper. Now for an elliptically anisotropic media we have $\eta = 0$ (in other words $\epsilon = \delta$) so that the above equation simplifies to:

$$k_z = \sqrt{\frac{\omega^2}{v^2} - (k_x^2+k_y^2)(1+2\epsilon)}. \tag{3}$$

Thus in 3-D the vertical wavenumber for the full Double Square Root (DSR) form of the elliptically anisotropic migration operator is:

$$k_z = \sqrt{\frac{\omega^2}{v(\mathbf{s},z)^2} - (k_{sx}^2+k_{sy}^2)(1+2\epsilon)} + \sqrt{\frac{\omega^2}{v(\mathbf{r},z)^2} - (k_{rx}^2+k_{ry}^2)(1+2\epsilon)}. \tag{4}$$

where $\mathbf{k_s}(k_{sx},k_{sy})$ is the source wavenumber vector and $\mathbf{k_r}(k_{rx},k_{ry})$ is receiver wavenumber vector. The equivalent form in midpoint-offset coordinates can be obtained by using the following simple transformations between the wavenumbers:

$$\mathbf{k_s} = \frac{\mathbf{k_m} - \mathbf{k_h}}{2}, \tag{5}$$

$$\mathbf{k_r} = \frac{\mathbf{k_m} + \mathbf{k_h}}{2}. \tag{6}$$

where $\mathbf{k_m}(k_{mx}, k_{my})$ is the midpoint wavenumber vector and $\mathbf{k_h}(k_{hx}, k_{hy})$ is the offset wavenumber vector. Substituting these transformations in equation (4) gives the vertical wavenumber for the elliptically anisotropic migration operator in midpoint-offset coordinates

$$k_z = \sqrt{\frac{\omega^2}{v(\mathbf{s},z)^2} - \frac{1}{4}\left\{(k_{mx}-k_{hx})^2 + (k_{my}-k_{hy})^2\right\}(1+2\epsilon)} + \sqrt{\frac{\omega^2}{v(\mathbf{r},z)^2} - \frac{1}{4}\left\{(k_{mx}+k_{hx})^2 + (k_{my}+k_{hy})^2\right\}(1+2\epsilon)} \tag{7}$$

The Common Azimuth downward continuation operator introduces a reduction in the dimensionality of the dataset by evaluating the new wavefield at a subsequent depth step only along the offset azimuth of the data in the previous depth step. The downward continuation operator (Biondi and Palacharla, 1996) can be expressed as:

$$\begin{aligned} P_{z+\Delta z}\left(\omega, \mathbf{k_m}, k_{x_h}, y_h = 0\right) &= \int_{-\infty}^{+\infty} dk_{y_h} P_z\left(\omega, \mathbf{k_m}, k_{x_h}, y_h = 0\right) e^{-ik_z \Delta z} \\ &= P_z\left(\omega, \mathbf{k_m}, k_{x_h}, y_h = 0\right)\left\{\int_{-\infty}^{+\infty} dk_{y_h} e^{-ik_z \Delta z}\right\} \\ &\approx P_z\left(\omega, \mathbf{k_m}, k_{x_h}, y_h = 0\right) A\left(\omega, \mathbf{k_m}, k_{x_h}\right) e^{-i\hat{k_z} \Delta z}. \end{aligned} \tag{8}$$

Since the common azimuth data is independent of k_{hy}, the integral can be pulled inside and analytically approximated by the stationary phase method. The stationary path approximation for the above operator can be found by setting the derivative of the wavenumber k_z with respect to k_{hy} to zero. This gives:

$$\hat{k}_{hy} = k_{my} \frac{\sqrt{\frac{\omega^2}{v(\mathbf{r},z)^2} - \frac{1}{4}(k_{mx}+k_{hx})^2(1+2\epsilon)} \mp \sqrt{\frac{\omega^2}{v(\mathbf{s},z)^2} - \frac{1}{4}(k_{mx}-k_{hx})^2(1+2\epsilon)}}{\sqrt{\frac{\omega^2}{v(\mathbf{r},z)^2} - \frac{1}{4}(k_{mx}+k_{hx})^2(1+2\epsilon)} \pm \sqrt{\frac{\omega^2}{v(\mathbf{s},z)^2} - \frac{1}{4}(k_{mx}-k_{hx})^2(1+2\epsilon)}} \tag{9}$$

As in the case of the isotropic Common Azimuth migration operator, the above equation has two solutions. In choosing between these two solutions, we consider the limiting case of the in-line offset wavenumber (k_{hx}) equal to zero. In this case, one of the solution diverges while the other one, which has a minus sign on the numerator, goes to zero. We accept this solution. This gives the stationary path approximation for an elliptically anisotropic media. Hence, the new vertical wavenumber, $\hat{k_{ze}}$ for elliptically anisotropic media is evaluated along the stationary path given in equation(9) and is equal to:

$$\hat{k}_{ze} = DSR[\omega, \mathbf{k}_m, k_{hx}, \hat{k}_{hy}, z] \tag{10}$$

STATIONARY PATH AND THE CONSTRAINTS ON THE RAY DIRECTIONS

In this section we show that the stationary path approximation derived in the previous section (equation (9)) is equivalent to imposing the constraint that the source and receiver rays must

be coplanar. For this constraint to hold, the following relation must be satisfied among the ray parameters:

$$\frac{p_{ry}}{p_{sy}} = \frac{p_{rz}}{p_{sz}}. \tag{11}$$

where (p_{sx}, p_{sy}, p_{sz}) are the rays downward propagating the sources and (p_{rx}, p_{ry}, p_{rz}) are the rays downward propagating the receivers. Applying the transformation from wavenumbers to ray parameter using the relation $\mathbf{p} = \mathbf{k}\omega$ to equation (3) we have:

$$p_z = \sqrt{\frac{\omega^2}{v^2} - \omega^2(p_x^2 + p_y^2)(1+2\epsilon)}. \tag{12}$$

Substituting equation (12) in equation (11) and after some algebra we get:

$$\frac{p_{ry} - p_{sy}}{p_{ry} + p_{sy}} = \frac{\sqrt{\frac{1}{v^2} - p_{rx}^2(1+2\epsilon)} - \sqrt{\frac{1}{v^2} - p_{sx}^2(1+2\epsilon)}}{\sqrt{\frac{1}{v^2} - p_{rx}^2(1+2\epsilon)} + \sqrt{\frac{1}{v^2} - p_{sx}^2(1+2\epsilon)}}. \tag{13}$$

Substituting the following relations in equation(13) gives the stationary path approximation derived in the previous section given by equation (9):

$$p_{sx} = \frac{k_{mx} - k_{hx}}{2\omega}, \tag{14}$$

$$p_{sy} = \frac{k_{my} - k_{hy}}{2\omega}, \tag{15}$$

$$p_{rx} = \frac{k_{mx} + k_{hx}}{2\omega}, \tag{16}$$

$$p_{ry} = \frac{k_{my} + k_{hy}}{2\omega}. \tag{17}$$

VTI COMMON AZIMUTH WITH BOUNDS

In this section, we derive an analytical form for the Common Azimuth migration operator for VTI media. As before, we start with the dispersion relation given by Alkhalifah (1998), now represented in terms of ray parameters:

$$p_z = \frac{1}{v}\sqrt{\frac{1-(1+2\epsilon)(p_x^2+p_y^2)v^2}{1-2\eta(1+2\delta)(p_x^2+p_y^2)v^2}}. \tag{18}$$

Using the geometrical constraints on the ray path for Common Azimuth migration (equation(11)) and after some simplifications, we get:

$$a_0 p_{sy}^4 + a_1 p_{ry}^4 + a_2 p_{ry}^2 + a_3 psy^2 = 0. \tag{19}$$

where

$$a_0 = 2\eta(1+2\delta)v_s^4, \tag{20}$$

$$a_1 = -2\eta(1+2\delta)v_r^4, \tag{21}$$

$$a_2 = v_r^2\left\{1-2\eta(1+2\delta)v_r^2 p_{rx}^2 - (1+2\epsilon)p_{rx}^2 v_s^2\right\}, \tag{22}$$

$$a_3 = -v_s^2\left\{1-2\eta(1+2\delta)v_s^2 p_{sx}^2 - (1+2\epsilon)p_{sx}^2 v_r^2\right\}. \tag{23}$$

Note that equation (19) is a quartic equation in both k_{hy} and k_{my}. This equation might be solved numerically for k_{hy} for given k_{my} values. But we want to have a closed form analytical solution. Rewriting equation (19) in a more suitable form, we get:

$$\begin{aligned} &v_r^2 p_{ry}^2\left\{1-2\eta(1+2\delta)v_r^2 p_{rx}^2 - 2\eta(1+2\delta)v_r^2 p_{ry}^2\right\} - \\ &v_s^2 p_{sy}^2\left\{1-2\eta(1+2\delta)v_r^2 p_{sx}^2 - 2\eta(1+2\delta)v_r^2 p_{sy}^2\right\} \quad -A_0 + A_1 = 0. \end{aligned} \tag{24}$$

where

$$A_0 = v_r^2 pry^2(1+2\epsilon)p_{sx}^2 v_s^2, \tag{25}$$

$$A_1 = v_s^2 p_{sy}^2(1+2\epsilon)p_{rx}^2. \tag{26}$$

Considering the first term in the curly bracket on the RHS of equation(24), we observe that in order to drop the fourth order term in p_{ry}, we need:

$$1-2\eta(1+2\delta)v_r^2 p_{rx}^2 >> 2\eta(1+2\delta)v_r^2 p_{ry}^2. \tag{27}$$

This can be rewritten as:

$$1-2\eta(1+2\delta)sin^2\theta_x >> 2\eta(1+2\delta)\sin^2\theta_y. \tag{28}$$

Recognizing that $\sin^2\theta$ is bounded in the interval $(0,1)$, we can write:

$$1 >> 4\mid \eta(1+2\delta)\mid . \tag{29}$$

Thus, we obtain a bound on η as:

$$\mid \eta \mid << \frac{1}{4(1+2\delta)} \approx \frac{1}{4}. \tag{30}$$

A similar analysis can be carried out for the second term in curly brackets on the RHS of equation (24) for dropping the fourth order term in p_{sy}, which again gives the same bound on η. Thus for VTI media, when the above bound holds, we can drop the fourth order terms in equation (19) giving:

$$\frac{p_{ry}}{p_{sy}} = \frac{\sqrt{\frac{1}{v_r^2} - \left\{(1+2\epsilon)p_{rx}^2 + 2\eta(1+2\delta)\frac{v_s^2}{v_r^2}p_{sx}^2\right\}}}{\sqrt{\frac{1}{v_s^2} - \left\{(1+2\epsilon)p_{sx}^2 + 2\eta(1+2\delta)\frac{v_r^2}{v_s^2}p_{rx}^2\right\}}} \tag{31}$$

Now using equations (14) to (17), we get:

$$\frac{\hat{k}_{hy}}{k_{my}} = \frac{A-B}{A+B}, \tag{32}$$

where

$$A = \sqrt{\frac{\omega^2}{v_r^2} - \frac{1}{4}\left\{(1+2\epsilon)(k_{mx}+k_{hx})^2 + 2\eta(1+2\delta)\frac{v_s^2}{v_r^2}(k_{mx}-k_{hx})^2\right\}}, \tag{33}$$

and

$$B = \sqrt{\frac{\omega^2}{v_s^2} - \frac{1}{4}\left\{(1+2\epsilon)(k_{mx}-k_{hx})^2 + 2\eta(1+2\delta)\frac{v_r^2}{v_s^2}(k_{mx}+k_{hx})^2\right\}}. \tag{34}$$

This equation gives an analytical form of the stationary path approximation for VTI media. As before, the vertical wavenumber, $\hat{k}_{zvti}$, is evaluated along this stationary path as:

$$\hat{k}_{zvti} = DSR[\omega, \mathbf{k}_m, k_{hx}, \hat{k}_{hy}, z] \tag{35}$$

Note that when $\eta = 0$, meaning for elliptically anisotropic media equation (34), reduces to equation (9) derived earlier for elliptically anisotropy media.

ERROR ANALYSIS

In this section, we compare the accuracy of the approximated analytical stationary path approximation for VTI media with the one obtained by numerically solving the full quartic equation for different η values (top panel of Figures 1-3). From the plots, we observe that the approximated analytical equation has similar accuracy as the one obtained by solving the quartic equation. Even when the η value exceeds the bound that was given in the previous section, the relative error is still sufficiently small. This indicates that our approximation should hold for a wide range of η values. The middle panel of Figures 1-3 shows the relative error between the isotropic and the analytically derived anisotropic stationary path. The bottom panels of figures 1-3 show the vertical wavenumbers computed for isotropic and anisotropic media for different η values. It can be seen that there are significant differences between the anisotropic and isotropic k_z values which, if ignored, will lead to significant mispositioning of migrated events.

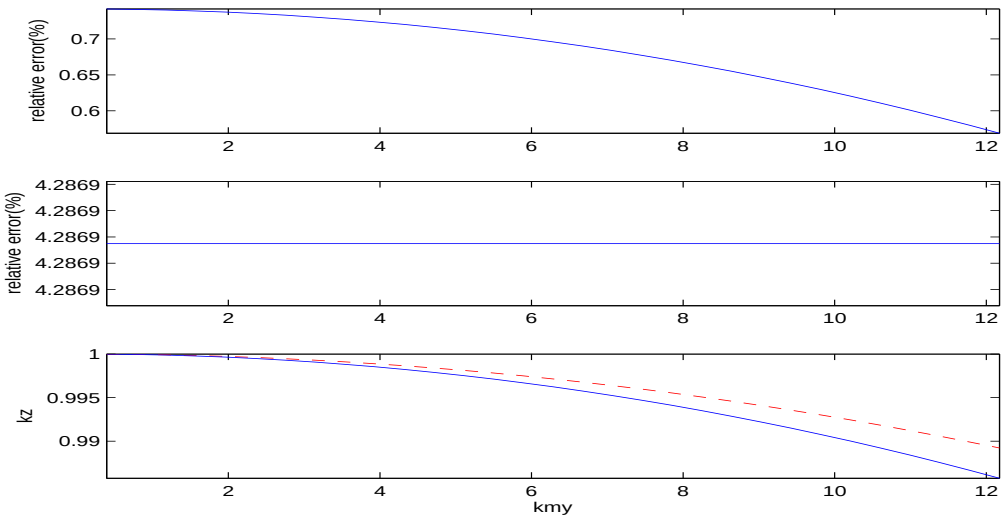

Figure 1: Relative Error plots for η = 0.08, relative error in k_{hy} between analytical and quartic solutions (top panel), relative error between analytical anisotropic and isotropic k_{hy} (middle panel), relative error between anisotropic (solid) and isotropic (dashed) k_z (bottom panel) ssen-eta08 [CR]

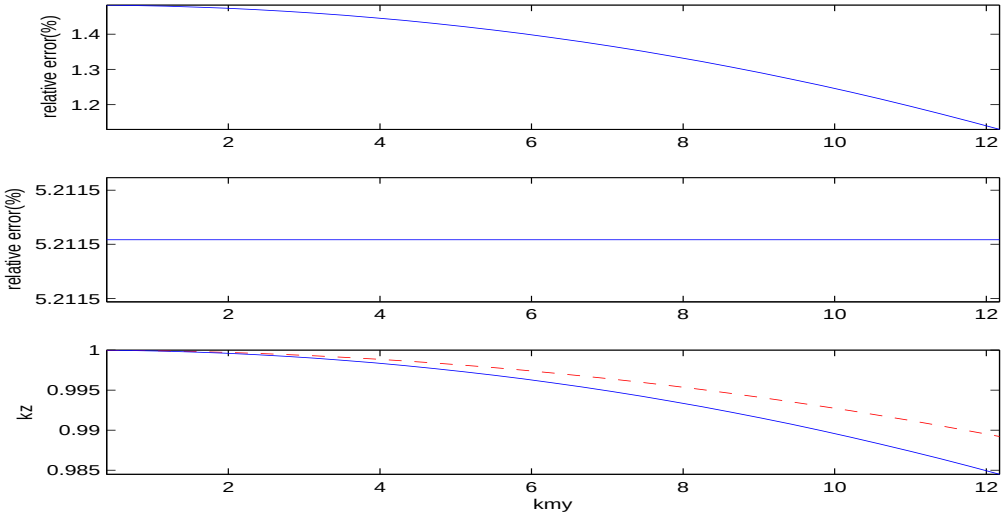

Figure 2: Relative error plots for η = 17, relative error in k_{hy} between analytical and quartic solutions (top panel), relative error between analytical anisotropic and isotropic k_{hy} (middle panel), relative error between anisotropic (solid) and isotropic (dashed) k_z (bottom panel) ssen-eta17 [CR]

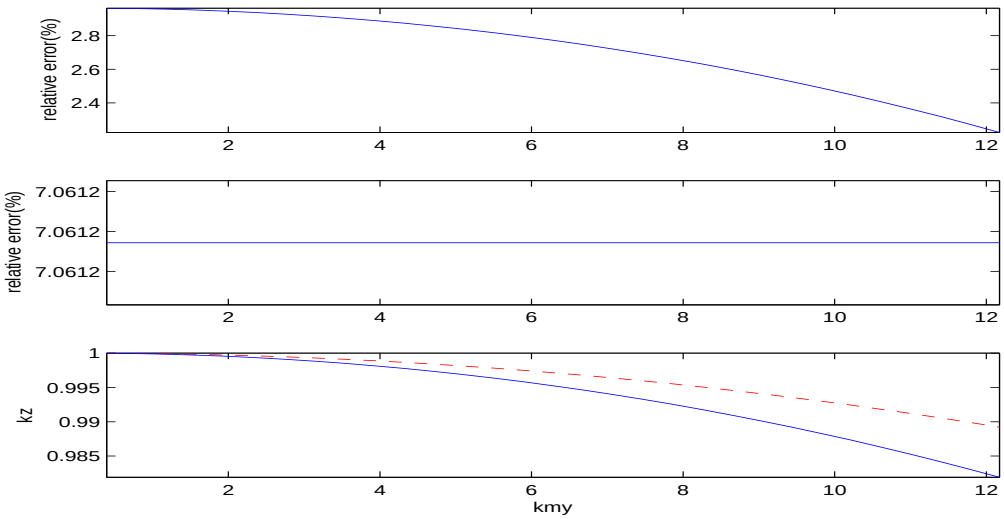

Figure 3: Relative error plots for $\eta = 0.33$, relative error in k_{hy} between analytical and quartic solutions (top panel), relative error between analytical anisotropic and isotropic k_{hy} (middle panel), relative error between anisotropic (solid) and isotropic (dashed) k_z (bottom panel) ssen-eta33 [CR]

3-D IMPULSE RESPONSES

In this section, we compare the 3-D impulse responses of the anisotropic Common Azimuth migration operator with the corresponding isotropic one. For this paper, we consider impulse responses for elliptical anisotropy only. The vertical P wave velocity in the medium is 2000 m/s. The anisotropic parameters ϵ and δ are both equal to 0.15. Figures 4 and 5 show in-line sections of the 3-D impulse responses for elliptically anisotropic and isotropic media respectively. These figures clearly show the difference of incorporating anisotropy into the Common Azimuth downward continuation operator, especially for energy propagating at moderate to steep angles. Figures 6 and 7 show cross-line sections of the 3-D impulse responses for elliptically anisotropic and isotropic media respectively. Again it can be seen that there are significant differences for energy propagating at moderate to steep angles once anisotropy is incorporated into the Common Azimuth operator. Finally, Figures 8 and 9 show depth slices of the 3-D impulse responses for elliptically anisotropic and isotropic media respectively. Again, we also observe significant differences between the two depth slices, especially the more elliptical nature of the depth slice for the anisotropic operator.

CONCLUSION

We have derived a Common Azimuth migration operator for elliptically anisotropic and VTI media. The elliptically anisotropic Common Azimuth migration operator is exact for all range

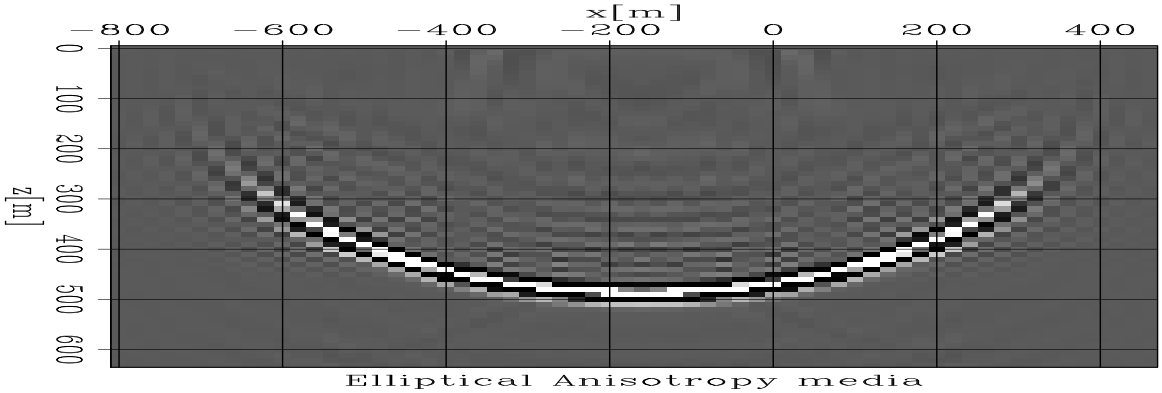

Figure 4: An inline slice of the 3D impulse response in an elliptically anisotropic media at $y = 0$ m. ssen-aniso15_inline [CR]

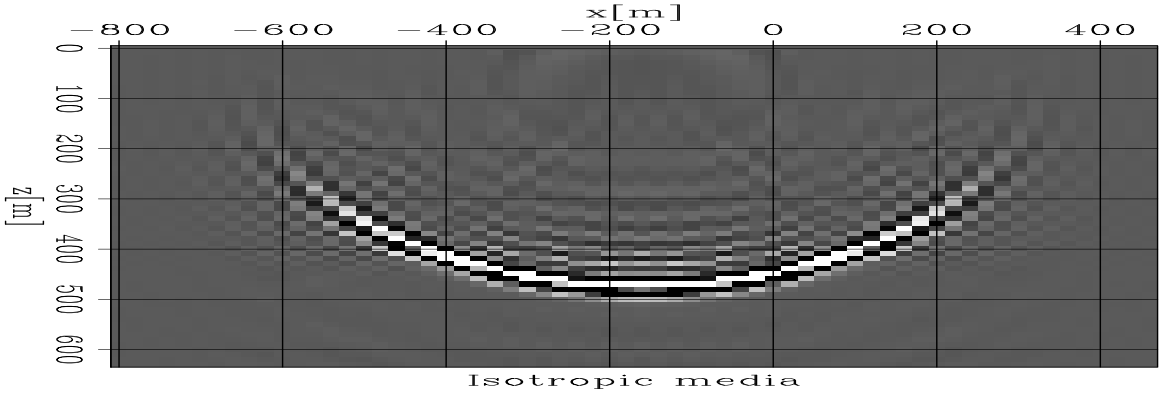

Figure 5: An inline slice of the 3D impulse response in an isotropic media at $y = 0$ m ssen-iso_inline [CR]

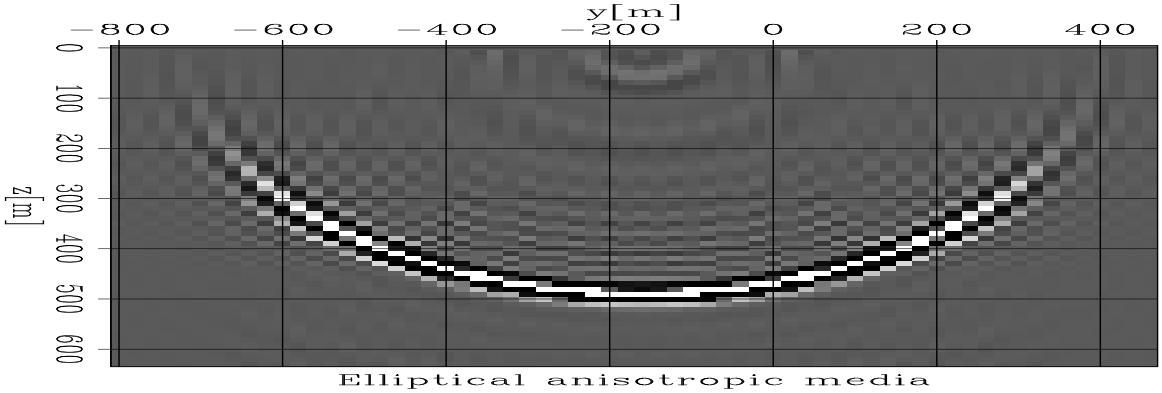

Figure 6: A cross-line slice of the 3D impulse response in an elliptically anisotropic media at $x = 0$ m ssen-aniso15_xline [CR]

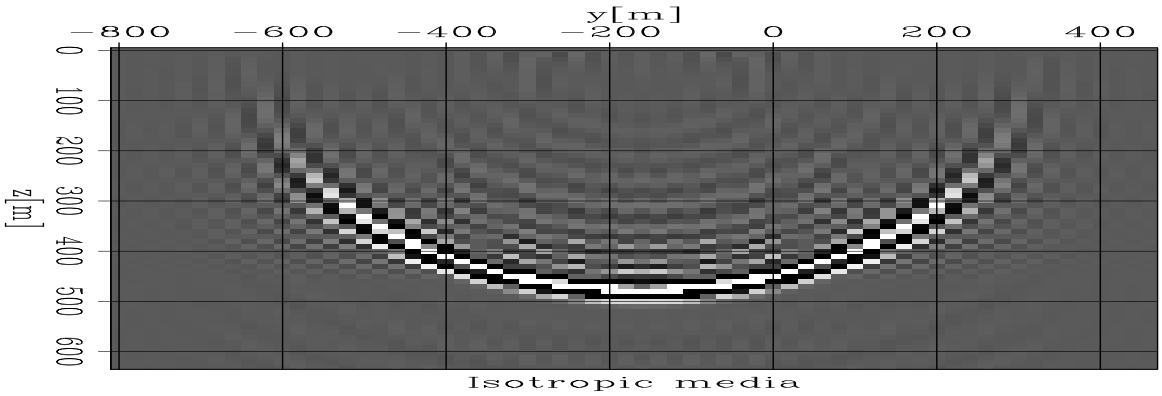

Figure 7: A cross-line slice of the 3D impulse response in an isotropic media at $x = 0$ m ssen-iso_xline [CR]

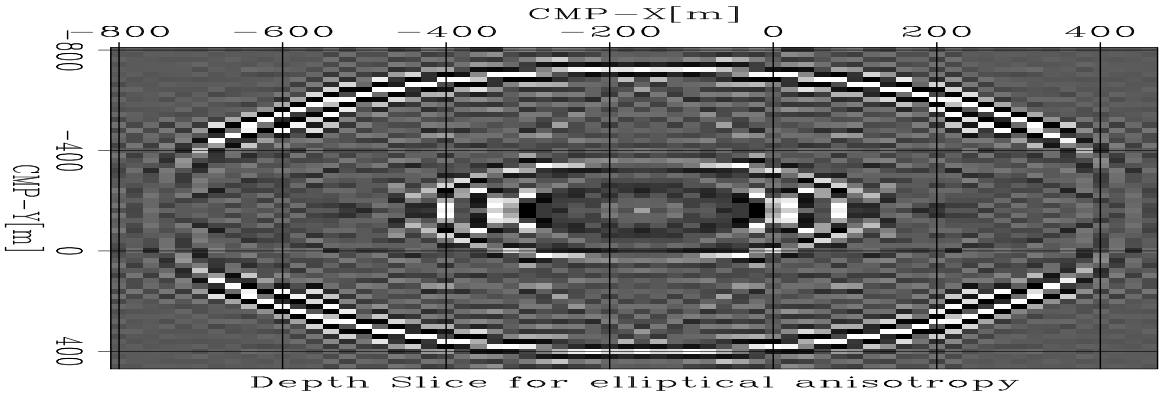

Figure 8: A horizontal slice of the 3D impulse response in an elliptically anisotropic media at a depth of $z = 600$ m. ssen-aniso15_depth_slice [CR]

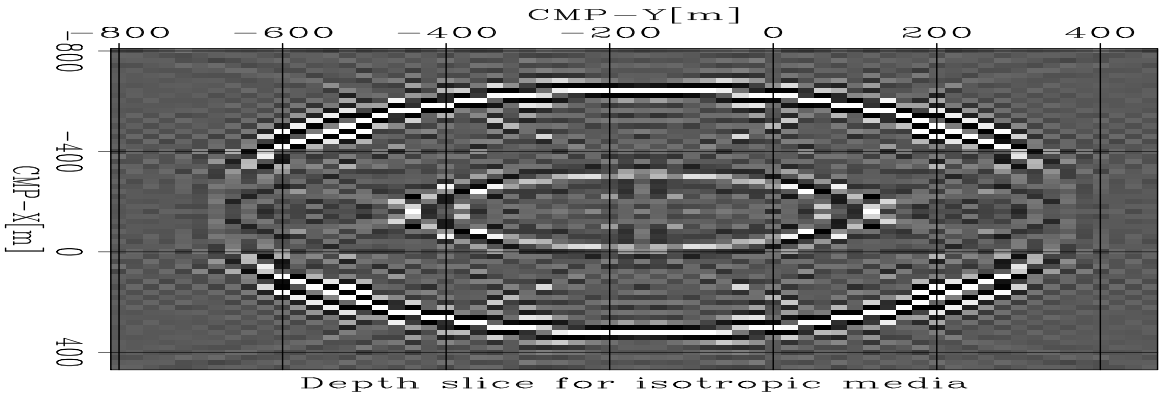

Figure 9: A horizontal slice of the 3D impulse response in an isotropic medium at $z = 600$ m. ssen-iso_depth_slice [CR]

of the governing anisotropic parameters, namely δ and ϵ. The Common Azimuth operator that we have developed for VTI media is a bounded one, meaning that it should be accurate within the certain bounds on the anisotropic parameters. But the error analysis indicates that even when these bounds are exceeded, the approximation is still good and the accuracy is comparable to the one obtained by solving the full quartic equation. 3-D impulse responses show that there are significant differences between the isotropic and anisotropic Common Azimuth downward continuation operator, which needs to be taken into account by the migration algorithm.

REFERENCES

Alkhalifah, T., 1998, An acoustic wave equation for anisotropic media: Geophysics, **65**, no. 4, 1239–1250.

Baumstein, A., and Anderson, J., 2003, Wavefield extrapolation in laterally varying vti media: 73rd Annual Internat. Mtg., Society Of Exploration Geophysicists, Expanded Abstract, 945–948.

Biondi, B., and Palacharla, G., 1996, 3-d prestack migration for common-azimuth data: Geophysics, **61**, no. 6, 1822–1832.

Ristow, D., and Ruhl, T., 1997, Migration in tranversely isotropic media using implicit operators: 67th Annual Internat. Mtg., Society Of Exploration Geophysicists, Expanded Abstracts, 1699–1702.

Rousseau, J. H. L., 1997, Depth migration in heterogeneous transversely isotropic media with the phase shift plus interpolation method.: 67th Annual Internat. Mtg., Society Of Exploration Geophysicists, Expanded Abstracts, 1703–1706.

Shan, G., and Biondi, B., 2004, Wavefield extrapolation in laterally varying tilted ti media: Report 117., Stanford Exploration Project, SEP, 1–9.

Uzcategui, O., 1995, 2-d depth migration in transversely isotropic media using explicit operators: Geophysics, **60**, no. 5, 1819–1829.

Zhang, J., Verschuur, D. J., and Wapenaar, C. P., 2001, Depth migration of shot records in heterogeneously transversely isotropic media using optimum explicit operators: Geophysical Prospecting, **49**, no. 4, 287–289.